

## Suitable pyrolysis model for physics-based bushfire simulation

Rahul Wadhvani<sup>1,2</sup>, Duncan Sutherland<sup>1,2,3</sup>, Khalid Moinuddin<sup>1,2</sup>

<sup>1</sup>Centre for Environmental Safety and Risk Engineering, Victoria University

Melbourne, VIC-3030, Australia

<sup>2</sup>Bushfire and Natural Hazards CRC

Melbourne, VIC-3002, Australia

<sup>3</sup>Department of Mechanical Engineering, University of Melbourne

Melbourne, VIC-3052, Australia

### Abstract

Models for the thermal degradation (or pyrolysis) of solid fuel are fundamental to the physics-based simulation of grassfires. The pyrolysis process affects the combustion process and therefore the simulated flame, which defines the fire front. There are two competing models: a simple linear parameterisation and a non-linear Arrhenius model. The present work appraises these two models for Lucerne hay (a cured herbaceous fuel) to test their suitability for bushfire simulation. Thermogravimetric analysis and differential scanning calorimetry of Lucerne hay is conducted to measure the parameters required for the simulation. Simulations of pyrolysis are carried out using both the linear and single effective Arrhenius models, and compared with the experimental results. For this fuel, the linear model provides better agreement with the experimental data than the Arrhenius model. Hence, the linear model would be more suitable for large-scale wildfire simulation.

### 1 Introduction

Wildfire (or bushfire) is a global natural disaster which causes economic and ecological damage of worth billions of dollars each year. Australia is dominated by grass pasture lands which are significantly different from forest litter fuels. To study how fire propagates in a bushfire, physics-based fire models [1] are ideal for research purposes. They simulate the behaviour of the fire by solving mass, energy, and momentum conservation equations. Pyrolysis is an integral part of physics-based models to simulate wildfires [1] and combustion which represents the fire front [2]. Both forest and grass fuels exhibit variation in material thermophysical and chemical properties. They show complicated multiple step reaction kinetics of thermal degradation [3], variation in fuel properties with locations and season [4], and intra-species variation [5]. To understand the fire propagation the pyrolysis of forest fuels must be modelled [2]. There are two competing models for pyrolysis: linear [2,6], and Arrhenius [7]. These models appraised using the pyrolysis of Lucerne hay (LuH) (also called Alfalfa, *Medicago satvia*) in this study. LuH is one of the animal feedstock crops grown in Victoria, Australia. LuH selected to minimise the effect of site variation and increase reproducibility of this experimental work.

### 2 Numerical Model

Wildland-urban-interface Fire Dynamics Simulator (WFDS)-an extension of Fire Dynamics Simulator (FDS) is an open-source physics-based CFD fire model to simulate fire propagation as a thermally driven flow [8]. Currently, it is integrated as a vegetation sub-model in FDS [8]. Mell *et al.* [2,9] showed the capability of WFDS to simulate grassfire and crown fire. WFDS has two ways to define vegetation fuels: (a) the boundary fuel method, where fuel is defined in bulk layer e.g. grassland and is smaller than the grid size [2]; (b) the fuel element method, where fuel such as Douglas trees are defined by particles in the same size of the numerical grid elements [9]. For large-scale fire modelling, such as grassland it is appropriate to use the boundary fuel method. To use the boundary fuel method, a pyrolysis model is still required. The pyrolysis may be modelled as the linear model or the Arrhenius model. The two competing pyrolysis model are discussed below.

#### 2.1 Linear model

The simple linear model [6] divides the mass loss rate of vegetation into three sections: (a) a step-change mass loss of moisture at 373K, (b) a linear rate of pyrolysis reaction ( $\dot{w}_{pyr\_Lin}$ ) (Equation 1), and (c) a negligible char mass loss rate. The important pyrolysis step is

$$\dot{w}_{pyr\_Lin} = \frac{Q_{net} (T - T_0)}{h_{pyr} (T_f - T_0)}, \quad (1)$$

where  $Q_{net}$  is the net input heat to the material (kJ/kg.K),  $h_{pyr}$  is the heat of pyrolysis reaction (kJ/kg),  $T_0$  and  $T_f$  are the initial and final temperature of the pyrolysis range, and  $T$  is sample temperature at any time  $t$ .  $T_0$  and  $T_f$  estimated from the thermogravimetric analyser (TGA), and  $h_{pyr}$  estimated from differential scanning calorimetry (DSC) for a particular material.  $Q_{net}$  requires measurement of specific heat capacity ( $C_p$ ) of the sample using a hot disk analyser (HDA).

#### 2.2 Arrhenius model

The Arrhenius model uses an Arrhenius equation to define the kinetics of the pyrolysis reaction (Equation 2). The default version of the model implemented in WFDS uses a single reaction kinetics based on Morvan & Dupuy [7]. A complex Arrhenius model [3] representing each component of the sample i.e. cellulose, hemicellulose, and lignin, is not considered because a single effective model for pyrolysis found

---

Corresponding author.

E-mail address: [rahul.wadhvani@live.vu.edu.au](mailto:rahul.wadhvani@live.vu.edu.au)

to be suitable for large-scale fires [7]. Furthermore, the scale of grassfires is in kilometres, and the grid size used for simulations for a 200x200m plot grassfires is typically of order centimetres [10] to metres [2]. This requires computation time from days to weeks in conjunction to huge computational resources. There is a requirement to reduce the computational time which further compels the use of a single effective Arrhenius model in simulation studies. The Arrhenius model requires the estimation of kinetic parameters: Arrhenius frequency factor ( $A$  ( $s^{-1}$ )), the activation energy of the reaction ( $E$  (kJ/mol)), and reaction function ( $f(\alpha)$ ) [11]. The reaction function used in default model is reaction order model [11]. Vyazovkin *et al.* [11] suggested that, it is required to estimate the reaction function for the sample tested in TGA to choose appropriate kinetic parameters. Thus, the Arrhenius model is

$$\dot{w}_{pyrArr} = A e^{\frac{-E}{RT}} f(\alpha) . \quad (2)$$

A non-isothermal method in which sample heated at a constant heating rate chosen to estimate the kinetic parameters. Furthermore, this technique has more relevance in fire science than the isothermal method [12]. Following the ICTAC recommendation [11], the isoconversional technique using the Kissinger-Akahira-Sunose (KAS) equation [13] is used to estimate the activation energy of the sample. A plot of heating rate ( $\beta$ ) vs.  $1/T$  at various heating rate gives the activation energy at each isoconversional slope [11,14]. After the activation energy measurement, a master YZ plot [11] is used to select the appropriate  $f(\alpha)$ , and then estimate the value of  $A$ .

### 3 Sample preparation

The LuH sample divided into three sections: leaf section (LuL) (representing the top part of hay consisting only the leaf, blades, seeds); stem section (LuS) (representing the bottom part of hay consisting only the stem, and nodes); and a mixture section (LuM) (which contains a 50-50 wt.% of LuL and LuS). The samples before any test conditioned at 27°C and 50% relative humidity for more than 36h. The initial mass of sample used in TGA and DSC kept constant to  $7.5 \pm 0.01$ mg and evenly distributed. A constant initial sample mass allows the application of Hoffman and Pan's method [15], using DSC observations, to estimate heat of pyrolysis reaction [15].

A Mettler Toledo TGA/DSC 1 and a Mettler Toledo DSC 1, was used for the TGA and DSC experiments. The sample was tested from 30-900°C in an inert atmosphere of nitrogen at 20ml/min gas flow rate for TGA, for a wide range of heating rate (5, 7.5, 10, 20, 50, 100 K/min). The large range of heating rate considered here was chosen to match the heating rate expected in wildfires. The effect of material size and flow rate of the carrier gas found to be negligible on the TGA results [14]. The DSC experiments were conducted at similar conditions to the TGA, except the temperature range was 30-500°C, due to the limitations of the equipment and the sample holder. The Mettler Toledo DSC was calibrated using a standard sapphire disk supplied by Mettler Toledo.

A Thermtest TPS 500 HDA was used to estimate bulk material specific heat capacity using the transient plane source method [15]. Material specific heat is required for the WFDS simulation using the boundary fuel method. A powdered sample of LuM size 0.2-0.6mm with porosity 0.39 [16] was used to ensure repeatability of the experiment and minimise the effect of the random size of pore spaces in the sample.

## 4 Results

### 4.1 Experimental Results

Figures 1 & 2, show the mass loss thermogram and rate of fractional conversion for LuL, LuS, and LuM at a representative heating rate of 20 K/min. From Fig. 2, it is visible that there is the presence of two shoulder peaks: 190-240°C (associated with hemicellulose) and 370-490°C (associated with lignin).  $T_0$  and  $T_f$  required for the linear model are estimated by visual inspection of Fig. 1 & 2. The  $T_0$  and  $T_f$  are observed to be 393K and 633K respectively.

The presence of these shoulder peaks relative to the main peak of cellulose for LuL is found to be similar to the eucalyptus leaves, and pine needles studied in [14]. KAS methodology [13] is used to estimate the activation energy of the species as a function of conversion [11,14]. The activation energy as a function of fractional conversion ( $\alpha$ ) in the pyrolysis region shown in Fig. 3. It is visible that the activation energy varies with the fractional conversion, which is quite different from timber [11,14] but like litters materials [5,14]. The variation in LuH components suggests a multi-step reaction model corresponding to each component (cellulose, hemicellulose, and lignin). The activation energy for LuS and LuM is linearly increasing with fractional conversion. However, the variation in LuL is different to previous observations for leaves [5,14]. Braga *et al.* [17] observed the change in activation energy for elephant grass in the range of 186-279 kJ/mol. They also observed a similar variation of activation energy with fractional conversion as observed for LuL. The range of variation in activation energy  $\sim 100$ kJ/mol is of the same order as obtained for elephant grass and forest litter materials [5,14,17]. However, for a grassfire simulation, it is reasonable to assume the applicability of a single effective pyrolysis model, due to constraint such as computational grid size, temporal and spatial variability in the vegetation, and a desire to reduce computation speed.

Finally, after estimating activation energy, the reaction model ( $f(\alpha)$ ) and corresponding Arrhenius frequency factor ( $A$ ) are estimated (Vyazovkin *et al.* [11] describe this process in detail). We applied a truncated Sestak-Berggren model [10] and obtained John-Mehl-Avrami (JMA, with exponent  $n = 4$ ) [11,14] model to be most appropriate for our data. That is,

$$f(\alpha)_{JMA(n=4)} = 4(1 - \alpha)[- \ln(1 - \alpha)]^{3/4} . \quad (3)$$

The KAS method is also used to estimate activation energy of moisture evaporation using the default reaction model [7]. Table 1 details the estimated kinetic parameters for LuH components. Furthermore, DSC was used to estimate the heat of pyrolysis required in the linear model. The experiment was performed with the same initial sample mass used in the TGA experiments so as to apply Hoffman & Pan's method [15]. The area between the data and calibration curves in the pyrolysis temperature range (obtained from Fig. 2) gives an estimate for the heat of the pyrolysis reaction. This is shown as a shaded region in Fig. 4, a positive value shows endothermic process. The Fig. 4 shows the second of the two-endothermic process: (1) moisture loss, (2) pyrolysis process; the curve is not horizontal due to inclined calibration curve.

The estimated values of the  $h_{pyr}$  are susceptible to the small inter-species variation of the samples affecting the computed area under the curve. Hence, the experiments are repeated ten times for consistent and repeatable observations. Most of the computed area under the curve from Fig. 4, estimates the heat of pyrolysis in the range of 525-575 kJ/kg. However, values in the range of 400-720 kJ/kg were also observed showing a probable variation in the estimation. Hence, a sensitivity

analysis for the heat of pyrolysis on the simulations is conducted later to understand the impact of the variation.

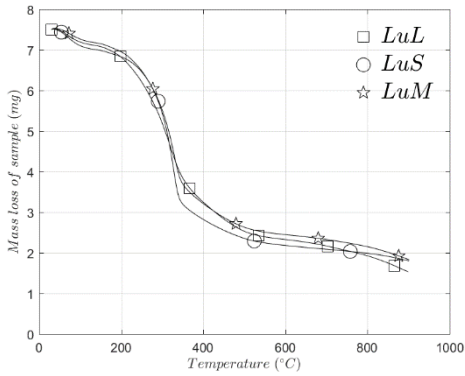


Figure 1: Mass loss thermogram for LuH components observed in the inert atmosphere of nitrogen in TGA at 20 K/min

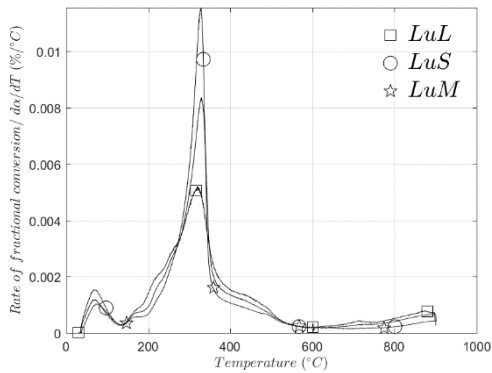


Figure 2: Rate of fractional conversion for LuH components in the inert nitrogen atmosphere at 20 K/min

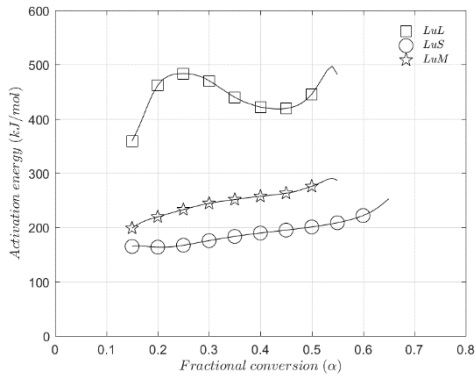


Figure 3: Activation energy as a function of fractional conversion ( $\alpha$ ) for LuH components by KAS

Variable	LuL	LuS	LuM
Density (kg/m <sup>3</sup> )	397.88	497.43	447.66
$A_{H_2O}$ (K <sup>1/2</sup> s <sup>-1</sup> )	1.17e+8 <sup>a</sup>	4.45e+6 <sup>a</sup>	1.62e+7 <sup>a</sup>
$E_{H_2O}$ (kJ/mol)	61.67	48.60	55.20
$A_{Spec}$ (s <sup>-1</sup> )	2.3e+34 <sup>a</sup>	2.65e+16 <sup>a</sup>	1.27e+22 <sup>a</sup>
$E_{Spec}$ (kJ/mol)	418.33	218.19	270.02

<sup>a</sup> estimated at 20 K/min

Table 1: Estimated kinetic parameters for LuH components

Heat capacity is measured as a function of temperature in the range of 30-150°C. A linear relation of  $C_p$  (kJ/kg.K) observed with temperature ( $T_{HDA}$  (K)) with  $r^2 = 0.883$ . Discrepancies in the fit are due to changes in  $C_p$  after the moisture loss at 100°C. This is similar to the moisture effects observed by Bakar [14] for pine timber when tested from 30-225°C. Also, similar linear relations of heat capacity with temperature were observed for pine needles [16], for biomass [17], and for wood [18]. The linear equation of  $C_p$  at initial relative humidity of 50% is

$$C_p = 0.0096T_{HDA} - 1.802 \quad (4)$$

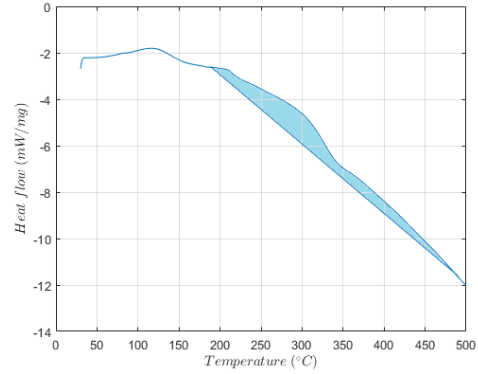


Figure 4: Heat flow of LuL observed in the inert nitrogen condition in DSC at 20 K/min

## 4.2 Simulated results

Simulations of the thermogravimetric experiments are carried out using Wildland-urban interface Fire Dynamic Simulator (WFDS) version 6.0.0. The simulation domain is  $x = -0.005, 0.005$ ,  $y = -0.005, 0.005$ ,  $z = 0, 0.01$  (m) and the vegetation patch on  $z = 0$  is  $x = -0.0025, 0.0025$ , and  $y = -0.00125, 0.00125$  (m). The boundary of the domain is assumed to be radiant panels which heats from 30-900°C to match the heating rate of experiment. The fuel loading (without moisture) is 0.5411 kg/m<sup>2</sup>; the vegetation height is 0.004 m; the vegetation density is defined in Table 1.

The linear model simulates the moisture evaporation section as a step change at 100°C [6] and hence, thermal degradation simulated from 120-900°C. Figure 5 shows the comparison between the experimental fractional mass loss observed in TGA and simulated fractional mass loss using WFDS with the linear model. Figure 6 shows a similar comparison using the Arrhenius model. It is quite visible from Fig. 5 & 6 that the linear model simulates the pyrolysis section 220-360 °C accurately.

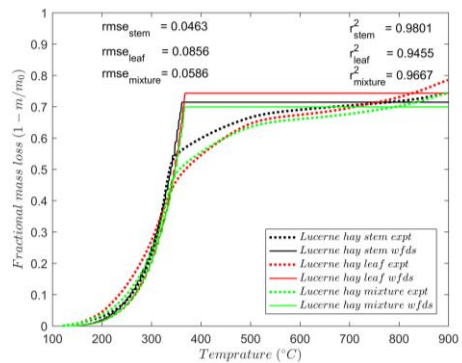


Figure 5: Fractional mass loss comparison for experimental & simulated case for LuH using the linear model at  $\beta=20$  K/min

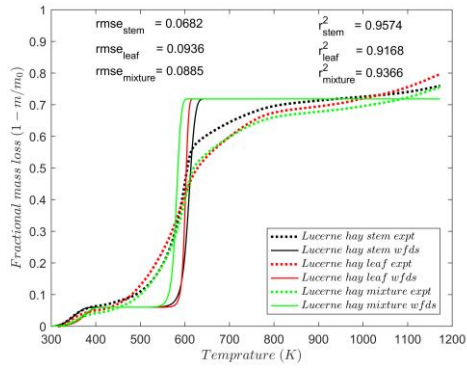


Figure 6: Fractional mass loss comparison for experimental & simulated case for LuH using the Arrhenius model at  $\beta=20$  K/min

Similarly, in the Arrhenius model there is a good prediction for moisture section. While in the pyrolysis section, the Arrhenius model does a poor job due to the use of a single best-fit model for a complex multi-step thermal degradation reaction [11,12]. Hence, the value of combined effect results similar value of root mean square error (rmse).

Figure 7 shows the sensitivity of the linear model with the variation in  $h_{pyr}$  for LuM at  $\beta=20$  K/min. The result show a maximum rmse = 0.0728 when  $h_{pyr}$  varied in  $\pm 30\%$  while the rmse is 0.0546 when the mean  $h_{pyr}$  is 550 kJ/kg, obtained from DSC. The variation in  $h_{pyr}$  observed in DSC does not show significant impact on the accuracy of the linear model.

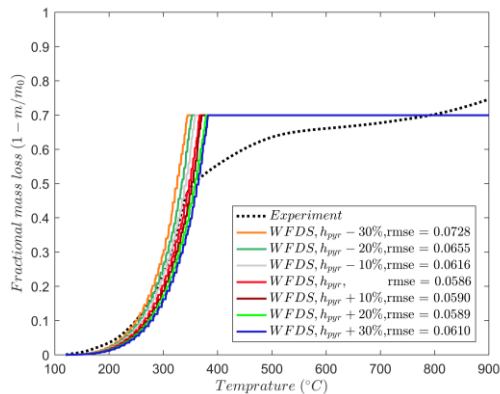


Figure 7: Sensitivity analysis for heat of pyrolysis for LuM at  $\beta=20$  K/min

## 5 Conclusions

The present work appraises two competing models, namely the linear and Arrhenius models, for pyrolysis in physics-based fire simulations of fires in herbaceous fuels. The linear model shows perform better than the single step Arrhenius model for pyrolysis at microscale (e.g. TGA). The results also show that linear model is fairly independent of the estimation and inter-species variation observed in DSC measurement. Further, it also shows that it is independent on LuH components, which suggests the usage of one  $h_{pyr}$  value to represent LuH vegetation. However, further verification and validation of these models at medium- to larger-scale samples, i.e. cone calorimeter, room-scale, are required to test the model applicability for large-scale bushfire simulation. Also, it will be required to test the applicability of these models for forest litters which are significantly different from herbaceous fuels like LuH.

## 6 Acknowledgment

We would like to acknowledge the Bushfire and Natural Hazard Cooperative Research Centre (BNHCRC), Melbourne, Australia for providing us financial support to carry out this work. We also like to thank Mr. Lyndon Macindoe and Mr. Philip Dunn for technical support and sample collection.

## References

- [1] A.L. Sullivan, Int. J. Wildland Fire 18 (2009) 349-68.
- [2] W. Mell, M. A. Jenkins, J. Gould, P. Cheney, Int. J. Wildland Fire 16 (2007) 1-22.
- [3] H. Niu, N. Liu, Effect of Particle Size on Pyrolysis Kinetics of Forest Fuels in Nitrogen, Fire Saf. Sci., 11, 2014, p. 1393-405.
- [4] D.H. Ashton, Aust. J. Bot. 23 (1975) 413-33.
- [5] O.P. Korobeinichev, A.A. Paletsky, M.B. Gonchikzhapov, I.K. Shundrina, H. Chen, N. Liu, Procedia Eng. 62 (2013) 182-93.
- [6] D. Morvan, J. Dupuy, Combust. Flame 138 (2004) 199-210.
- [7] D. Morvan, J. Dupuy, Combust. Flame 127 (2001) 1981-94.
- [8] K. McGrattan, S. Hostikka, J. Floyd, R. McDermott, C. Weinschenk, K. Overholt, Fire Dynamics Simulator Technical Reference Guide Volume 1: Mathematical Model, National Institute of Standards and Technology, Special Publication 1018, Gaithersburg, MD, 2013, p. 149.
- [9] W. Mell, A. Maranghides, R. McDermott, S.L. Manzello, Combust. Flame 156 (2009) 2023-41.
- [10] D. Morvan, S. Meradji, W. Mell, Fire Saf. J. 58 (2013) 195-203.
- [11] S. Vyazovkin, A.K. Burnham, J.M. Criado, L.A. Pe' rez-Maqueda, C. Popescu, N. Sbirrazzuoli, Thermochem Acta. 520 (2011) 1-19.
- [12] F. Richter, G. Rein, Fire Saf. J. 91 (2017) 191-9
- [13] H.E. Kissinger, Anal. Chem. 29 (1957) 1702-6
- [14] R. Wadhvani, D. Sutherland, K.A.M. Moinuddin, P. Joseph, J. Therm. Anal. Cal. (2017) (doi: 10.1007/s10973-017-6512-0)
- [15] A.S.A. Bakar, *Characterization of Fire Properties for Coupled Pyrolysis and Combustion Simulation and Their Optimised Use*, PhD Thesis, Victoria University, Melbourne, Australia, 2016.
- [16] N. Ouchiyama, T. Tanaka, Ind. Eng. Chem. Fundam 23(4) (1984) 490-3
- [17] R. Braga, D. Melo, F. Aquino, J. Freitas, M. Melo, J. Barros, M. Fontes, J. Therm. Anal. Cal. 115(2) (2014) 1915-20.
- [18] R. A. Susott, Forest Sci. 28 (1982) 839-51.
- [19] W.C.R. Chan, M. Kelbon, B. B. Krieger, Fuel, 64 (1985) 1505-13.
- [20] K. Radmanović, I. Đukić, S. Pervan, Drvna industrija, 65 (2014) 151-7.